HHS Public Access

Author manuscript

Toxicol Lett. Author manuscript; available in PMC 2020 June 01.

Published in final edited form as:

Toxicol Lett. 2019 June 01; 307: 11–16. doi:10.1016/j.toxlet.2019.02.015.

Insights into the transcriptional regulation of the anthracycline reductase *AKR7A2* in human cardiomyocytes

Adolfo Quiñones-Lombraña[1], **Amy Intini**[1], and **Javier G. Blanco**[1,*]

[1]Department of Pharmaceutical Sciences, University at Buffalo, The State University of New York (SUNY), Buffalo, New York.

Abstract

Aldo-Keto Reductase Family 7 Member A2 (AKR7A2) is the most abundant anthracycline metabolizing enzyme in human myocardium. Myocardial AKR7A2 contributes to the synthesis of cardiotoxic C-13 anthracycline alcohol metabolites (e.g., doxorubicinol). The factors that govern the transcription of human *AKR7A2* in cardiomyocytes remain largely unexplored. In this study, we performed the functional characterization of the *AKR7A2* gene promoter in human AC16 cardiomyocytes. Experiments with gene reporter constructs and chromatin immunoprecipitation assays suggest that NF-κB binds to specific regions in the *AKR7A2* promoter. Doxorubicin treatment modified the cellular levels of NF-κB and the expression of *AKR7A2.* Moreover, doxorubicin treatment led to changes in the pattern of AKR7A2 phosphorylation status. Our results suggest that *AKR7A2* expression in human cardiomyocytes is mediated by NF-κB through conserved response elements in the proximal gene promoter region. This study provides the first insights into the functional characteristics of the human *AKR7A2* gene promoter.

Keywords

Aldo-Keto Reductase Family 7 Member A2 (AKR7A2); human cardiomyocytes; anthracyclines

1. Introduction

AKR7A2 (Aldo-Keto Reductase Family 7 Member A2) encodes a member of the Aldo-Keto Reductases (AKRs) superfamily of NAD(P)H linked oxidoreductases that reduce aldehydes and ketones to alcohols (Penning and Drury, 2007). Originally identified as the main enzyme responsible for the reduction of succinic semialdehyde (SSA) to γ-hydroxybutyrate (GHB) in human brain, AKR7A2 metabolizes a broad range of endogenous and exogenous carbonyl-containing compounds, including the anticancer anthracyclines doxorubicin and

*Corresponding author at: Department of Pharmaceutical Sciences, University at Buffalo, The State University of New York, 470 Kapoor Hall, Buffalo, NY 14214 – 8033, USA, Phone: 716 - 645 – 4820, Fax: 716 - 829 – 6569, jgblanco@buffalo.edu.

CONFLICT OF INTEREST

The authors declare that there are no conflicts of interest.

daunorubicin (Bains et al., 2010; O'Connor et al., 1999; Quinones-Lombrana et al., 2014; Schaller et al., 1999). AKR7A2 is involved in cellular detoxification pathways through the metabolism of toxic aldehydes and interactions with other stress-responsive proteins such as cytoglobin (Li et al., 2012; Li et al., 2016).

Anthracyclines are widely used for the chemotherapy of a variety of solid and hematological cancers. The therapeutic potential of anthracyclines is hampered by the dose-dependent relation with irreversible cardiomyopathy leading to congestive heart failure (Grenier and Lipshultz, 1998; McGowan et al., 2017; Volkova and Russell, 2011). The risk for anthracycline-related cardiotoxicity is modified by total cumulative exposure, younger age at cancer diagnosis, radiation therapy to the chest region, trisomy 21 (Down syndrome), and female sex (Hefti and Blanco, 2016; Lipshultz et al., 1995; O'Brien et al., 2008; Von Hoff et al., 1979). It has been postulated that specific myocardial AKRs including AKR7A2 contribute to anthracycline-related cardiotoxicity through the synthesis of cardiotoxic C-13 anthracycline alcohol metabolites (e.g., doxorubicinol and daunorubicinol) (Mushlin et al., 1993; Olson et al., 1988; Piska et al., 2017; Stewart et al., 1993). From a toxicodynamic perspective, the 2-electron reduction of the parent anthracycline catalyzed by myocardial AKRs (e.g., AKR67A2) and carbonyl reductases (CBRs) is an activation step, shown by a significant body of evidence demonstrating that the resulting C-13 alcohol metabolites accumulate in long-term reservoirs that are key to the pathogenesis of cardiomyopathy (Menna et al., 2012; Minotti et al., 2010; Mordente et al., 2009; Olson et al., 1988).

Recently we used classification and regression tree models (CART) to predict the synthesis of cardiotoxic daunorubicinol in human myocardium (Hoefer et al., 2016). Results from this analysis suggested that myocardial AKR7A2 protein content is an important variable for determining the synthesis of daunorubicinol. AKR7A2 is the most abundant anthracycline reductase in human myocardium accounting for up to 36% of the total anthracycline reductase content (Quinones-Lombrana et al., 2014). The expression of *AKR7A2* mRNA and AKR7A2 protein in myocardium exhibits considerable interindividual variability (*AKR7A2* mRNA: ~89-fold, AKR7A2 protein: ~13-fold) (Quinones-Lombrana et al., 2014).

Different transcription enhancer elements have been previously identified in the promoter region of *AKR7A2* (Penning and Drury, 2007). A recent report has shown that knockdown of the nuclear factor erythroid 2–related factor 2 (Nrf2) results in a 35% decrease in *AKR7A2* mRNA expression in human hepatic cells (HepG2) (Li et al., 2015). Although the main mechanisms that mediate anthracycline-cardiotoxicity have been characterized in detail, there is a remarkable paucity of data regarding the molecular factors that dictate the variable expression and bioactivating activity of prominent AKRs/CBRs in human myocardium. This limitation hampers our ability to predict responses at the organ level during pharmacotherapy with anthracyclines under different pathophysiological conditions. The goal of the present study was to analyze the transcriptional regulation of *AKR7A2* in a model cell line representative of adult human ventricular cardiomyocytes. Complementary studies were performed to assess the effect of doxorubicin on the expression of *AKR7A2* in cardiomyocytes.

2. Material and Methods

2.1. Cell culture

AC16 cells (Human cardiomyocytes, Millipore Sigma, Burlington, MA) were routinely cultured in 100 X 15 mm tissue culture dishes (Santa Cruz Biotechnology, Dallas, TX) using DMEM/F12 (Life Technologies, Carlsbad, CA) supplemented with 10% (v/v) heat-inactivated fetal bovine serum (Sigma-Aldrich, St. Louis, MO), 100 U/ml penicillin (Life Technologies), and 100 μg/ml streptomycin (Life Technologies). Cell cultures were grown and maintained at low passage numbers ($n \leq 12$) using standard incubation conditions at 37°C, 5% CO_2, and 95% relative humidity.

2.2. Reagents

Dimethyl sulfoxide (DMSO) and phosphate-buffered saline (PBS) were purchased from Sigma-Aldrich. Doxorubicin hydrochloride was purchased from Cayman Chemicals (Ann Arbor, MI) and stock solutions (10 mM) were prepared in DMSO and diluted to working concentrations in serum-free media.

2.3. AKR7A2 reporter constructs and site-directed mutagenesis

CpG-free pCpGL basic vector was kindly donated by Dr. Michael Rehli (University Hospital Regensburg, Regensburg, Germany) (Klug and Rehli, 2006). A 522 base pairs (bp) DNA fragment from human *AKR7A2* (−1 to −522 bp upstream the translation initiation codon A $_{+1}$TG) was amplified by PCR with specific primers (Table 1). The fragment was ligated into the *Hin*dIII site of the pCpGL basic vector. Deletions produced by PCR were cloned into the *Hin*dIII site of the pCpGL basic vector. NF-κB and xenobiotic response element consensus binding sequences (*XRE*) were mutated with the QuikChange Lightning site-directed mutagenesis kit (Agilent, Santa Clara, CA). All constructs were verified by DNA sequencing.

2.4. Transfections

Twenty-four hours prior to transfections, AC16 cells were plated in 48-well plates. Cells were transfected with the *AKR7A2* luciferase reporter construct or the backbone vector (100 ng) plus the internal control plasmid pRL-TK (10 ng) using Lipofectamine 3000 transfection reagent (Life Technologies) in serum-free media. Twenty four hours post transfection, cultures were washed once with PBS; cells were lysed in freshly diluted passive lysis buffer (50 μl/well, Promega, Madison, WI) by incubating plates at room temperature on a shaker at 200 rpm for 20 min. Luciferase reporter gene activities were determined with the Dual-Luciferase Reporter Assay System (Promega) per the manufacturer's instructions. Light intensity was measured in a Synergy HT luminometer equipped with proprietary software for data analysis (BioTek, Winooski, VT). Corrected firefly luciferase activities were normalized to renilla luciferase activities and expressed relative to the averaged activity of the $^{-}{}_{522}$*AKR7A2*-pCpGL construct, which was assigned an arbitrary value of 100 Relative Luciferase Units (RLUs). Experiments were performed in triplicates.

2.5. Chromatin immunoprecipitation

Assays were performed using the ChIP-IT Enzymatic Shearing kit (Active Motif, Carlsbad, CA) according to the manufacturer's instructions. Briefly, cells were cross-linked with 1% formaldehyde at room temperature for 5 min, repeatedly washed with ice-cold phosphate buffer, and lysed using a Dounce homogenizer followed by centrifugation. The nuclear pellet was suspended in enzymatic shearing mixture and digested at 37°C for 12 min to shear the DNA. A fraction of the mixture of protein-DNA complex was used as "input DNA". Sheared chromatin (15 μg) was then incubated overnight at 4°C with protein G magnetic beads and 2 μg of anti-NF-κB p65 antibody (sc-8008 X, Santa Cruz Biotechnology, Dallas, TX) or normal mouse IgG. Immuno-precipitated DNA was eluted from protein G beads, then cross-linking was reversed and DNA was purified. A 191-bp fragment of the *AKR7A2* proximal promoter region was amplified by PCR with the following primers: $AKR7A2_{\text{ChIPf}}$: 5′-CCTCGTCCCACGATATCGC-3′; $AKR7A2_{\text{ChIPr}}$: 5′-CCTTGACCCAGAAGCTGGG-3′. PCR products were electrophoresed on a 2% agarose gel stained with SyBr Safe (Life technologies) for visualization.

2.6. Cell viability

The viability of doxorubicin treated AC16 cells was determined using the luciferase-based CellTiter-Glo Luminescent Cell Viability Assay (Promega) as per the manufacturer's instructions. Briefly, twenty-four hours prior to viability assays, AC16 cells were plated in 96-well plates and treated with doxorubicin as described. Measurements were made in triplicates.

2.7. Quantification of AKR7A2 mRNA expression

Total RNA was isolated with Trizol reagent (Life technologies). *AKR7A2* mRNA expression was analyzed by qRT-PCR with specific primers ($AKR7A2_{\text{forward}}$: 5′-GGCCTCTCCAACTATGCTAG-3′; $AKR7A2_{\text{reverse}}$: 5′-GGCATAGAACCTCAGTCCAAAG-3′) following MIQE guidelines as previously reported (Bustin et al., 2009; Quinones-Lombrana et al., 2014). Briefly, total RNA (25 ng) was reverse transcribed and amplified with the iTaq Universal SYBR Green One-Step Kit (Bio Rad). *AKR7A2* and *ACTB* (reference gene, $ACTB_{\text{forward}}$: 5′-GGACTTCGAGCAAGAGATGG-3′, and $ACTB_{\text{reverse}}$: 5′-AGCACTGTGTTGGCGTACAG-3′) were amplified in parallel in a CFX96 Touch Real-Time PCR Detection System (Bio-Rad, Hercules, CA) with the following cycling parameters: 50°C for 10 min (reverse transcription), 95°C for 1 min, followed by 40 cycles of 95°C for 15 s, 56°C for 30 s and 72°C for 30 s.

2.8. Immunoblotting

For the analysis of AKR7A2 and NF-κB protein expression, AC16 cells were homogenized in phosphate buffer supplemented with protease inhibitor (Life technologies) using zirconium oxide beads and a Bullet Blender homogenizer (Next Advance, Averill Park, NY). The resulting homogenates were centrifuged at 8000 rpm for 3 min at 4°C, and the supernatants were collected for protein analysis. Total protein concentration was determined with the bicinchoninic acid assay kit (Life technologies) as per the manufacturer's protocol.

Proteins were reduced with NuPAGE LDS sample buffer containing NuPAGE sample reducing agent (Life technologies), and denatured by heating at 70°C for 10 min. Total protein (15 μg) was separated by gel electrophoresis using NuPAGE Novex 4 – 12% Bis-Tris precast gels, and transferred onto PVDF membranes using the iBlot Gel Transfer Device (Life technologies). Membranes were blocked with 5% non-fat milk in 0.2% Tween 20-PBS for 1 hour at room temperature and then probed with specific monoclonal antihuman AKR7A2 or NF-κB-p65 antibodies (sc-100503 and sc-8008, respectively; Santa Cruz Biotechnology) overnight at 4°C. Next, membranes were incubated with mouse IgG kappa binding protein (m-IgGκ BP) conjugated to horseradish peroxidase (Santa Cruz Biotechnology) for 1.5 hours at room temperature. To normalize for protein loading, membranes were stripped with Restore Western Blot Stripping Buffer (Life technologies) and re-probed with anti-ACTB antibody (sc-8432; Santa Cruz Biotechnology). Immunoreactive bands were visualized with the Pierce ECL Western blot substrate (Life technologies) in a ChemiDoc XRS+ imager (Bio-Rad, Berkeley, CA). Densitometric analyses were performed using Image Lab software (Bio-Rad).

2.9. Phosphatase treatment.

Identification of AKR7A2 phosphorylation status was assessed by incubation of 15 μg of AC16 total cellular proteins with 25 units of calf intestine alkaline phosphatase (Promega) in a 20 μl reaction volume containing 50 mM Tris/HCl (pH 9.3), for 1 hour at 37°C. Changes in the electrophoretic mobility of AKR7A2 due to protein dephosphorylation were detected by immunoblotting as described.

2.10. Data analysis

The presence of transcription factor binding motifs in the *AKR7A2* promoter region was examined with a combination of algorithms including PhysBinder and ConTra v.3. PhysBinder uses an approach based on the incorporation of nucleotide position dependencies related to the three dimensional structure of DNA while ConTra v.3. utilizes experimentally validated transcription factor binding sites derived from ChIP-Seq data released by the ReMap project (Broos et al., 2013; Kreft et al., 2017). Statistics were computed with Excel 2013 (Microsoft Office; Microsoft, Redmond, WA) and GraphPad Prism version 4.03 (GraphPad Software Inc., La Jolla, CA). The D'Agostino-Pearson test was used to analyze the normality of datasets. The Student's t-test was used to compare group means. Data are expressed as the mean ± standard deviation (SD). Differences between means were considered significant at $p \leq 0.05$.

3. Results and Discussion

First, we identified the minimal promoter region of human *AKR7A2*. To test for gene promoter activity, a 522 bp fragment upstream the $A_{+1}TG$ codon corresponding to the putative *AKR7A2* promoter region was cloned into a pCpGL luciferase reporter vector. The resulting construct ($_{-522}$*AKR7A2*-pCpGL) was transiently transfected into cultures of AC16 human cardiomyocytes. The $_{-522}$*AKR7A2*-pCpGL construct exerted significant gene promoter activity in cardiomyocytes (Fig 1A). Three shorter constructs (421, 339, and 250 bp long) were generated to further explore the activity of the *AKR7A2* gene promoter. Gene

reporter assays showed that the $_{-522}$*AKR7A2*-pCpGL and the $_{-421}$*AKR7A2*-pCpGL constructs exhibited similar gene promoter activities (100.0 ± 14.8 vs. 109.5 ± 31.9 RLUs respectively; Student's t test $p = 0.351$; Fig. 1A). Further deletions of the *AKR7A2* promoter region led to significant decreases in luciferase activity ($_{-339}$*AKR7A2*-pCpGL: 32.6 ± 7.3 RLUs, Student's t test $p < 0.001$; $_{-250}$*AKR7A2*-pCpGL: 17.7 ± 3.7 RLUs, Student's t test $p < 0.001$; Fig. 1A). These results suggest that the −522 to −339 bp region is key for the basal expression of *AKR7A2* in human cardiomyocytes.

In silico analysis of the *AKR7A2* gene promoter revealed the presence of a conserved binding motif for the transcription factor NF-κB in the −341 to −330 bp region. In addition, a canonical xenobiotic response element (*XRE*) was identified in the −134 to −130 bp proximal promoter region. The contribution of these binding motifs to basal gene promoter activity in cardiomyocytes was examined by performing site directed mutagenesis. Mutation of the *XRE* core nucleotide sequence had no significant effect on basal *AKR7A2* gene promoter activity when compared to the activity of the non-mutated *AKR7A2* promoter ($_{-522}$*AKR7A2*-pCpGL: 100.0 ± 14.8; $_{-522\text{m}XRE}$*AKR7A2*-pCpGL: 89.1 ± 24.2 RLUs; Student's t test $p = 0.214$; Fig. 1B). Mutation of the conserved NF-κB binding motif led to a 49% decrease in basal *AKR7A2* gene promoter activity (51.4 ± 16.8 RLUs; Student's t test $p < 0.001$, Fig. 1B). The presence of interactions between NF-κB and the proximal promoter region of *AKR7A2* in cardiomyocytes was examined by performing chromatin immunoprecipitation. Immunoprecipitation of cellular DNA with an anti-p65-NF-κB antibody allowed the PCR amplification of the *AKR7A2* promoter fragment containing the NF-κB binding motif (Fig. 1C). This result suggests that NF-κB directly binds to the proximal promoter of *AKR7A2* to mediate basal gene expression in AC16 cardiomyocytes.

Doxorubicin activates the NF-κB signaling pathway by inducing degradation of IκBα and production of NF-κB complexes that are capable of DNA binding (Esparza-Lopez et al., 2013; Ho et al., 2005; Wang et al., 2002). The activation of NF-κB by doxorubicin in various cell types is dependent upon incubation time and drug concentration (Chuang et al., 2002; Wang et al., 2002). Thus, we examined the impact of NF-κB on the expression of AKR7A2 in response to doxorubicin treatment. Treatments for 12 hours with 0.1 μM and 0.5 μM doxorubicin did not impact the expressions of NF-κB and AKR7A2 in cardiomyocytes, and had negligible effect on cellular viability (Figs. 2A and B). Next, the effect of the 12 hours treatments with doxorubicin was examined after a 24 hours incubation period in drug free media. At this time-point, cellular levels of NF-κB protein decreased by ~70% (0.1 μM) and ~80% (0.5 μM) while cell viabilities were ~70% (0.1 μM) and ~45% (0.5 μM. Figs. 2C and D). In line, *AKR7A2* mRNA levels were reduced by 68% (0.1 μM), and 77% (0.5 μM) (Fig. 3A). Interestingly, analysis of AKR7A2 protein expression showed an increase in the intensity of the 46 KDa band after exposure to 0.5 μM doxorubicin (Fig. 3B). It is known that doxorubicin activates the phosphorylation of multiple targets through generation of reactive oxygen species and activation of the serine–threonine protein kinase Akt (Kurz et al., 2004; Li et al., 2005). Treatment of cellular lysates with alkaline phosphatase decreased the intensity of the 46 KDa band which suggests the presence of phosphorylated AKR7A2 in cardiomyocytes exposed to doxorubicin (Fig. 3B). Little is known in regards to the effects of post translational modifications on the function of members of the aldo-keto reductase family. Varma et al. showed that AKR1B1, also known

as aldose reductase, is phosphorylated upon stimulation by protein kinase C (PKC), and that this modification is associated with increased levels of AKR1B1 in mitochondrial membranes (Varma et al., 2003). Analysis of subcellular fractions of SHSY-5Y neuroblastoma cells showed that a fraction of AKR7A2 protein may be located in the mitochondria (Weiner et al., 2009). Thus, it will be of interest to examine the dynamics of AKR7A2 phosphorylation with an emphasis on mitochondrial translocation in cardiomyocytes treated with anthracyclines (Berthiaume and Wallace, 2007; Cui et al., 2017; Wallace, 2003).

4. Conclusions

Our results suggest that *AKR7A2* expression in cardiomyocytes is mediated by NF-κB through conserved response elements in the proximal gene promoter region. Further studies are warranted to evaluate the role of AKR7A2 phosphorylation in response to the cardiotoxic activity of anthracyclines.

Acknowledgments

This study was supported by the National Institute of General Medical Sciences (award GM073646).

Abbreviations:

AKR1B1	aldo-keto reductase family 1 member B1
AKR7A2	aldo-keto reductase family 7 member A2
CART	classification and regression tree model
ChIP	chromatin immunoprecipitation
DMSO	dimethyl sulfoxide
GHB	γ-hydroxybutyrate
NAD(P)H	nicotinamide adenine dinucleotide phosphate
NF-κB	nuclear factor kappa-light-chain-enhancer of activated B cells
Nrf2	nuclear factor erythroid 2–related factor 2
PBS	phosphate buffered saline
PCR	polymerase chain reaction
RLU	relative luciferase units
SSA	succinic semialdehyde

References

Bains OS, Grigliatti TA, Reid RE, Riggs KW, 2010 Naturally occurring variants of human aldo-keto reductases with reduced in vitro metabolism of daunorubicin and doxorubicin. The Journal of pharmacology and experimental therapeutics 335, 533–545. [PubMed: 20837989]

Berthiaume JM, Wallace KB, 2007 Adriamycin-induced oxidative mitochondrial cardiotoxicity. Cell biology and toxicology 23, 15–25. [PubMed: 17009097]

Broos S, Soete A, Hooghe B, Moran R, van Roy F, De Bleser P, 2013 PhysBinder: Improving the prediction of transcription factor binding sites by flexible inclusion of biophysical properties. Nucleic acids research 41, W531–534. [PubMed: 23620286]

Bustin SA, Benes V, Garson JA, Hellemans J, Huggett J, Kubista M, Mueller R, Nolan T, Pfaffl MW, Shipley GL, Vandesompele J, Wittwer CT, 2009 The MIQE guidelines: minimum information for publication of quantitative real-time PCR experiments. Clin Chem 55, 611–622. [PubMed: 19246619]

Chuang SE, Yeh PY, Lu YS, Lai GM, Liao CM, Gao M, Cheng AL, 2002 Basal levels and patterns of anticancer drug-induced activation of nuclear factor-kappaB (NF-kappaB), and its attenuation by tamoxifen, dexamethasone, and curcumin in carcinoma cells. Biochemical pharmacology 63, 1709–1716. [PubMed: 12007574]

Cui L, Guo J, Zhang Q, Yin J, Li J, Zhou W, Zhang T, Yuan H, Zhao J, Zhang L, Carmichael PL, Peng S, 2017 Erythropoietin activates SIRT1 to protect human cardiomyocytes against doxorubicin-induced mitochondrial dysfunction and toxicity. Toxicol Lett 275, 28–38. [PubMed: 28456571]

Esparza-Lopez J, Medina-Franco H, Escobar-Arriaga E, Leon-Rodriguez E, Zentella-Dehesa A, Ibarra-Sanchez MJ, 2013 Doxorubicin induces atypical NF-kappaB activation through c-Abl kinase activity in breast cancer cells. Journal of cancer research and clinical oncology 139, 1625–1635. [PubMed: 23892407]

Grenier MA, Lipshultz SE, 1998 Epidemiology of anthracycline cardiotoxicity in children and adults. Semin Oncol 25, 72–85. [PubMed: 9768828]

Hefti E, Blanco JG, 2016 Anthracycline-Related Cardiotoxicity in Patients with Acute Myeloid Leukemia and Down Syndrome: A Literature Review. Cardiovasc Toxicol 16, 5–13. [PubMed: 25616318]

Ho WC, Dickson KM, Barker PA, 2005 Nuclear factor-kappaB induced by doxorubicin is deficient in phosphorylation and acetylation and represses nuclear factor-kappaB-dependent transcription in cancer cells. Cancer Res 65, 4273–4281. [PubMed: 15899819]

Hoefer C, Blair R, Blanco J, 2016 Development of a CART model to predict the synthesis of cardiotoxic daunorubicinol in heart tissue samples from donors with and without Down syndrome. Elsevier.

Klug M, Rehli M, 2006 Functional analysis of promoter CpG methylation using a CpG-free luciferase reporter vector. Epigenetics 1, 127–130. [PubMed: 17965610]

Kreft L, Soete A, Hulpiau P, Botzki A, Saeys Y, De Bleser P, 2017 ConTra v3: a tool to identify transcription factor binding sites across species, update 2017. Nucleic acids research 45, W490–W494. [PubMed: 28472390]

Kurz EU, Douglas P, Lees-Miller SP, 2004 Doxorubicin activates ATM-dependent phosphorylation of multiple downstream targets in part through the generation of reactive oxygen species. The Journal of biological chemistry 279, 53272–53281. [PubMed: 15489221]

Li D, Ferrari M, Ellis EM, 2012 Human aldo-keto reductase AKR7A2 protects against the cytotoxicity and mutagenicity of reactive aldehydes and lowers intracellular reactive oxygen species in hamster V79–4 cells. Chem Biol Interact 195, 25–34. [PubMed: 22001351]

Li D, Ma S, Ellis EM, 2015 Nrf2-mediated adaptive response to methyl glyoxal in HepG2 cells involves the induction of AKR7A2. Chem Biol Interact 234, 366–371. [PubMed: 25451587]

Li X, Lu Y, Liang K, Liu B, Fan Z, 2005 Differential responses to doxorubicin-induced phosphorylation and activation of Akt in human breast cancer cells. Breast Cancer Res 7, R589–597. [PubMed: 16168102]

Li X, Zou S, Li Z, Cai G, Chen B, Wang P, Dong W, 2016 The identification of human aldo-keto reductase AKR7A2 as a novel cytoglobin-binding partner. Cell Mol Biol Lett 21, 25. [PubMed: 28536627]

Lipshultz SE, Lipsitz SR, Mone SM, Goorin AM, Sallan SE, Sanders SP, Orav EJ, Gelber RD, Colan SD, 1995 Female sex and higher drug dose as risk factors for late cardiotoxic effects of doxorubicin therapy for childhood cancer. N Engl J Med 332, 1738–1743. [PubMed: 7760889]

McGowan JV, Chung R, Maulik A, Piotrowska I, Walker JM, Yellon DM, 2017 Anthracycline Chemotherapy and Cardiotoxicity. Cardiovasc Drugs Ther 31, 63–75. [PubMed: 28185035]

Menna P, Paz OG, Chello M, Covino E, Salvatorelli E, Minotti G, 2012 Anthracycline cardiotoxicity. Expert Opin Drug Saf 11 Suppl 1, S21–36.

Minotti G, Salvatorelli E, Menna P, 2010 Pharmacological foundations of cardiooncology. The Journal of pharmacology and experimental therapeutics 334, 2–8. [PubMed: 20335321]

Mordente A, Meucci E, Silvestrini A, Martorana GE, Giardina B, 2009 New developments in anthracycline-induced cardiotoxicity. Current medicinal chemistry 16, 1656–1672. [PubMed: 19442138]

Mushlin PS, Cusack BJ, Boucek RJ, Jr., Andrejuk T, Li X, Olson RD, 1993 Time-related increases in cardiac concentrations of doxorubicinol could interact with doxorubicin to depress myocardial contractile function. Br J Pharmacol 110, 975–982. [PubMed: 8298821]

O'Brien MM, Taub JW, Chang MN, Massey GV, Stine KC, Raimondi SC, Becton D, Ravindranath Y, Dahl GV, 2008 Cardiomyopathy in children with Down syndrome treated for acute myeloid leukemia: a report from the Children's Oncology Group Study POG 9421. J Clin Oncol 26, 414–420. [PubMed: 18202418]

O'Connor T, Ireland LS, Harrison DJ, Hayes JD, 1999 Major differences exist in the function and tissue-specific expression of human aflatoxin B1 aldehyde reductase and the principal human aldo-keto reductase AKR1 family members. The Biochemical journal 343 Pt 2, 487–504. [PubMed: 10510318]

Olson RD, Mushlin PS, Brenner DE, Fleischer S, Cusack BJ, Chang BK, Boucek RJ, Jr., 1988 Doxorubicin cardiotoxicity may be caused by its metabolite, doxorubicinol. Proceedings of the National Academy of Sciences of the United States of America 85, 3585–3589. [PubMed: 2897122]

Penning TM, Drury JE, 2007 Human aldo-keto reductases: Function, gene regulation, and single nucleotide polymorphisms. Arch Biochem Biophys 464, 241–250. [PubMed: 17537398]

Piska K, Koczurkiewicz P, Bucki A, Wojcik-Pszczola K, Kolaczkowski M, Pekala E, 2017 Metabolic carbonyl reduction of anthracyclines - role in cardiotoxicity and cancer resistance. Reducing enzymes as putative targets for novel cardioprotective and chemosensitizing agents. Invest New Drugs 35, 375–385. [PubMed: 28283780]

Quinones-Lombrana A, Ferguson D, Hageman Blair R, Kalabus JL, Redzematovic A, Blanco JG, 2014 Interindividual variability in the cardiac expression of anthracycline reductases in donors with and without Down syndrome. Pharm Res 31, 1644–1655. [PubMed: 24562808]

Schaller M, Schaffhauser M, Sans N, Wermuth B, 1999 Cloning and expression of succinic semialdehyde reductase from human brain. Identity with aflatoxin B1 aldehyde reductase. Eur J Biochem 265, 1056–1060. [PubMed: 10518801]

Stewart DJ, Grewaal D, Green RM, Mikhael N, Goel R, Montpetit VA, Redmond MD, 1993 Concentrations of doxorubicin and its metabolites in human autopsy heart and other tissues. Anticancer research 13, 1945–1952. [PubMed: 8297100]

Varma T, Liu SQ, West M, Thongboonkerd V, Ruvolo PP, May WS, Bhatnagar A, 2003 Protein kinase C-dependent phosphorylation and mitochondrial translocation of aldose reductase. FEBS Lett 534, 175–179. [PubMed: 12527382]

Volkova M, Russell R, 3rd, 2011 Anthracycline cardiotoxicity: prevalence, pathogenesis and treatment. Curr Cardiol Rev 7, 214–220. [PubMed: 22758622]

Von Hoff DD, Layard MW, Basa P, Davis HL, Jr., Von Hoff AL, Rozencweig M, Muggia FM, 1979 Risk factors for doxorubicin-induced congestive heart failure. Ann Intern Med 91, 710–717. [PubMed: 496103]

Wallace KB, 2003 Doxorubicin-induced cardiac mitochondrionopathy. Pharmacol Toxicol 93, 105–115. [PubMed: 12969434]

Wang S, Kotamraju S, Konorev E, Kalivendi S, Joseph J, Kalyanaraman B, 2002 Activation of nuclear factor-kappaB during doxorubicin-induced apoptosis in endothelial cells and myocytes is pro-apoptotic: the role of hydrogen peroxide. The Biochemical journal 367, 729–740. [PubMed: 12139490]

Weiner H, Duester G, Maser E, Plapp B, 2009 Enzymology and Molecular Biology of Carbonyl Metabolism Introduction. Chem-Biol Interact 178, 1–1. [PubMed: 19056364]

Highlights

- NF-κB binds to specific regions in the *AKR7A2* promoter in AC16 cardiomyocytes.
- Doxorubicin modifies cellular levels of NF-κB and the expression of AKR7A2.
- Doxorubicin changes AKR7A2 phosphorylation status in AC16 cells.

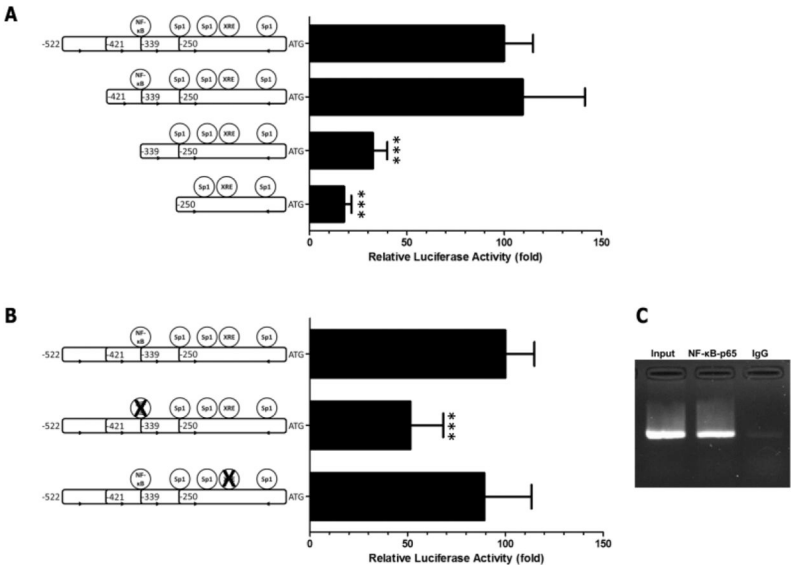

Fig. 1. Reporter gene activities of human *AKR7A2* promoter constructs.

(A) Luciferase activities of progressive *AKR7A2* deletion constructs in AC16 cardiomyocytes. Normalized luciferase activities were expressed relative to the values from the $_{-522}$*AKR7A2*-pCpGL construct, which was assigned an arbitrary value of 100. (B) Luciferase activities of mutated *AKR7A2* constructs. For each mutated construct, normalized luciferase activities were expressed relative to the values from the $_{-522}$*AKR7A2*-pCpGL construct, which was assigned an arbitrary value of 100. (C) Chromatin immunoprecipitation (ChIP) analysis of NF-κB binding to the *AKR7A2* promoter. Data represent the mean ± standard deviation of three independent experiments. *** $p < 0.001$ (Student's t-test).

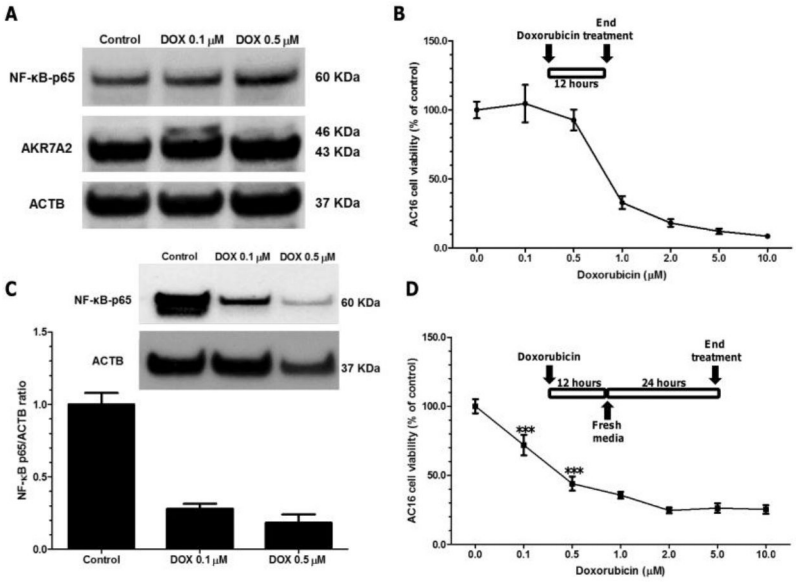

Fig. 2. Effects of doxorubicin treatment on cellular NF-κB and AKR7A2 protein levels.

(A) Representative immunoblot for NF-κB-p65 and AKR7A2 protein levels in AC16 cells treated with doxorubicin (0.1 μM and 0.5 μM) for 12 hours. (B) Viability of AC16 cells treated with doxorubicin for 12 hours. (C) Immunoblot analysis and densitometric results for the estimation of NF-κB-p65 protein levels in AC16 cells treated with doxorubicin (0.1 μM and 0.5 μM) for 12 hours followed by incubation in drug-free media for 24 hours. (D) Viability of AC16 cells treated with doxorubicin for 12 hours followed by incubation in drug free media for 24 hours. Data represent the mean ± standard deviation of three independent experiments. *** $p < 0.001$ (Student's t-test).

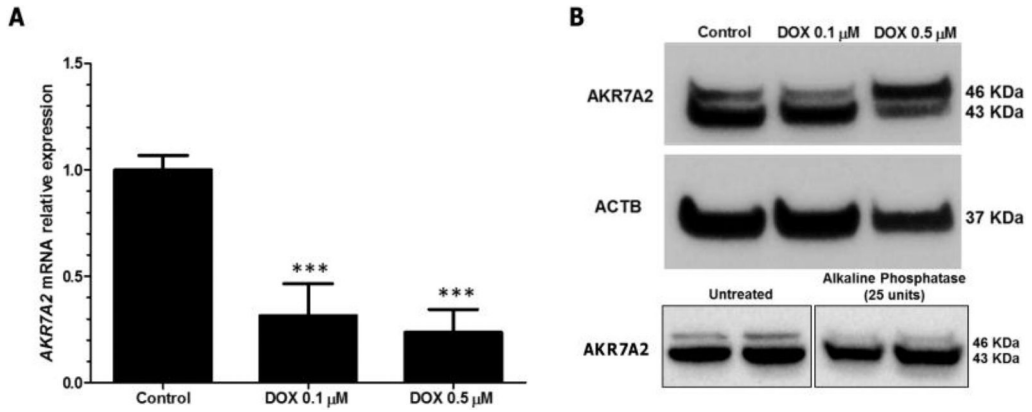

Fig. 3. Effect of doxorubicin treatment on *AKR7A2* mRNA expression and AKR7A2 protein phosphorylation.

(A) Effect of doxorubicin exposure of AC16 cells on *AKR7A2* mRNA levels. (B) Representative immunoblot showing AKR7A2 expression after doxorubicin exposure (0.1 μM and 0.5 μM) for 12 hours followed by 24 hours incubation in drug-free media. Bottom insert shows AKR7A2 gel mobility before and after dephosphorylation by alkaline phosphatase. Data represent the mean ± standard deviation of three independent experiments. *** $p < 0.001$ (Student's t-test).

Table 1.

List of primers used

AKR7A2$_{-522}$		5′-GCCATCAGATGCCAAGGGG-3′
AKR7A2$_{-421}$		5′-CTGCGGATTCCCGAGGGC-3′
AKR7A2$_{-339}$		5′- GACAGTCCAGCGGCCGG-3′
AKR7A2$_{-245}$		5′-GGTCCGGCTCACCACGTC-3′
AKR7A2r		5′- AGCAGCGGCGCCTGCGCG-3′
NF-κB mutant	Forward	5′- GAGGGCGCAGGAGCCAAAACAGTCCAGCGGCCG-3′
	Reverse	5′- CGGCCGCTGGACTGTTTTGGCTCCTGCGCCCTC-3′
XRE mutant	Forward	5′- GCAGGCCCCGCCCCCAAAACGCGCGCTG-3′
	Reverse	5′- CAGCGCGCGTTTTGGGGGCGGGGCCTGC-3′